



Multiplexed mycotoxins determination employing white light reflectance spectroscopy and silicon chips with silicon oxide areas of different thickness

Vasileios Anastasiadis^{a,b}, Georgios Koukouvinos^a, Panagiota S. Petrou^{a,*},
Anastasios Economou^b, James Dekker^c, Mikko Harjanne^c, Paivi Heimala^c,
Dimitris Goustouridis^d, Ioannis Raptis^d, Sotirios E. Kakabakos^a

^a Immunoassays-Immunoassays Lab, INRaSTES, NCSR "Demokritos", Aghia Paraskevi, 15310, Greece

^b Analytical Chemistry Lab, Department of Chemistry, University of Athens, Panepistimiopolis, Zografou, 15771, Greece

^c VTT Technical Research Centre of Finland Ltd., Espoo, FI-02150, Finland

^d ThetaMetrisis S.A, Athens, 12132, Greece

ARTICLE INFO

Keywords:

Multiplexed detection
Multi area reflectance spectroscopy
Aflatoxin B₁
Fumonisin B₁
Cereal samples

ABSTRACT

Biosensing through White Light Reflectance Spectroscopy (WLRs) is based on monitoring the shift of interference spectrum due to the binding reactions occurring on top of a thin SiO₂ layer deposited on a silicon chip. Multi-analyte determinations were possible through scanning of a single sensor chip on which multiple bioreactive areas have been created. Nonetheless, the implementation of moving parts increased the instrumentation size and complexity and limited the potential for on-site determinations. Thus, in this work, a new approach, which is based on patterning the sensor surface to create areas with different SiO₂ thickness, is developed and evaluated for multi-analyte determinations with the WLRs set-up. The areas of different thickness can be interrogated by a single reflection probe placed on a fixed position over the chip and the reflection spectrum recorded is deconvoluted to the spectra corresponding to each area allowing the simultaneous monitoring of the bio-reactions taking place at each one of them. The combination of different areas thickness was optimized using chips with two areas for single analyte assays. The optimum chips were then used for the simultaneous determination of two mycotoxins, aflatoxin B₁ and fumonisin B₁. A competitive immunoassay format was followed employing immobilization of mycotoxin-protein conjugates onto the SiO₂ of different thickness. It was found that the dual-analyte assays had identical analytical characteristics with the respective single-analyte ones. The detection limits achieved were 0.05 ng/mL for aflatoxin B₁ and 1.0 ng/mL for fumonisin B₁, with dynamic ranges extending up to 5.0 and 50 ng/mL, respectively. The sensor was also evaluated for the determination of the two mycotoxins in whole grain samples (wheat and maize). The extraction protocol was optimized and recoveries ranging from 85 to 115% have been determined. Due to lack of moving parts, the novel multi-analyte format is expected to considerably facilitate the built-up of a portable device for determination of analytes at the point-of-need.

1. Introduction

Label-free optical detection technologies offer a quite important advantage over their counterparts employing labels, since the lack of labels reduces the analysis cost and enables for direct detection of biomolecular reactions thus, making these technologies the number one candidate for application at the Point-of-Need (PoN) (Makarona et al., 2016).

The high potential for implementation of label-free detection concepts in PoN applications is the driving force for the research effort in this area and has led to the development of several methodologies relying on optical transducers which offer considerable advantages in terms of analysis duration, sensitivity, reproducibility, etc. (Chen et al., 2019). The label-free optical biosensing principles could be categorized in those relying on: a) planar waveguides (e.g., ring resonators, Mach-Zehnder interferometers, Young interferometer, etc.), where the

* Corresponding author. Immunoassay/Immunoassays Lab, Institute of Nuclear & Radiological Sciences & Technology, Energy & Safety, NCSR "Demokritos", GR-15310, Aghia Paraskevi, Greece.

E-mail address: ypetrou@rrp.demokritos.gr (P.S. Petrou).

<https://doi.org/10.1016/j.bios.2020.112035>

Received 31 October 2019; Received in revised form 3 January 2020; Accepted 16 January 2020

Available online 18 January 2020

0956-5663/© 2020 Elsevier B.V. All rights reserved.

in- and out-light coupling to the planar waveguiding structure raises obstacles for PoN applications (Kozma et al., 2014; Makarona et al., 2016), b) surface plasmon resonance (SPR), localized SPR (LSRP) and fiber-optic SPR (Zhou et al., 2019), or c) free space interference, e.g., biolayer interference (BLI) (Kamat and Rafique, 2017), reflectometric interference spectroscopy (RiFS) (Rau et al., 2014), 1- λ RiFS (Bleher et al., 2014), porous Si interferometry (Chen et al., 2019; Arshavsky-Graham et al., 2019) and white light reflectance spectroscopy (WLRS) (Koukouvinos et al., 2017a).

The last category offer certain advantages over the other optical technologies. For example, in the free-space interference concepts, the illumination of the sensing area is straightforward while the monitoring of the bioreaction is also easy through photodetectors and spectrometers. In addition, these transduction principles provide immunity to temperature variations and limited effect from the change in the refractive index of the sample under analysis, while the bio-chips are easy to be fabricated and of low-cost. Solutions based on these principles have already reached the market (e.g., by Pall, Biometrics, and Konica-Minolta). Nonetheless, the majority of the technologies offer single point measurements while for multi-analyte determinations either the reflection probe should scan an area where different recognition biomolecules have been immobilized onto spatially distinct positions (Koukouvinos et al., 2016, 2017b; Stavra et al., 2018) or multiple reflection probes should be employed (Kamat and Rafique, 2017). In both cases the effect on biosensor reader complexity and cost is pronounced.

In the present work, we introduce for the first time a novel concept of 3-D structuring of a transparent layer on Si substrate for the monitoring of multiple bioreactions with a single reflection probe and without any moving parts. This Multi Area Reflectance Spectroscopy (MARS) methodology widens the application of reflectometric technologies, such as WLRS (Koukouvinos et al., 2015, 2016, 2017b, 2018; Tsounidi et al., 2019), BLI (Kamat and Rafique, 2017) and RiFS (Rau et al., 2014; Bleher et al., 2014), without the need of a new reader. In all these technologies, a transparent layer produces an interference spectrum that is monitored through a reflection probe and a spectrometer. The growth of a biomolecular layer on top of the transparent layer causes red spectral shifts that are tracked by the spectrometer resulting in bioanalytical tools with high detection sensitivity and the ability to monitor the kinetics of the bioreaction in real-time. The fabrication of MARS transducers consists of a series of standard optical lithography steps, etching steps and thermal oxidation steps that allow for the realization of chips with closely spaced sensing areas with different but well-defined thicknesses of the transparent layer on top of the Si wafer. Each one of the sensing areas has adequate size to accommodate for immobilization of the biomolecules of interest and at the same time, the distance between them is small enough to facilitate the recording of the reflected light with the same reflection probe. The transparent layer implemented in the current work was silicon dioxide (SiO₂) that is patterned to two sensing areas of different thickness. Each sensing area was functionalized with a different mycotoxin-protein conjugate aiming to simultaneous determination of two mycotoxins, aflatoxin B1 and fumonisin B1, in cereal samples. The specific transducer configuration enabled the interrogation of both areas during the immunoreaction by a single reflection probe, thus abolishing the need for moving parts or employment of multiple probes as is the case in previous publications (Koukouvinos et al., 2016, 2017b; Stavra et al., 2018; Kamat and Rafique, 2017) based on reflectometric interference spectroscopy. In fact, the MARS reflectance spectrum comes from the two sensing areas plus the narrow sensing area between the sensing areas. Thus, the MARS reflectance spectrum can be considered as the sum of three reflectance spectra, the weight of which depends on each area. The fitting algorithm for the MARS reflectance spectrum takes into account the SiO₂ thickness of each sensing area and calculates independently the growth of the respective biomolecular adlayers.

Mycotoxins are poisonous secondary metabolites produced by fungi and often encountered in a great variety of food products including

cereals like maize, sorghum, pearl millet, rice and wheat, oilseeds, soybean, sunflower and cotton, spices like chilies, black pepper, coriander, turmeric and zinger, tree nuts such as almonds, pistachio, walnuts and coconut, and milk (Berthiller et al., 2013). They are very stable under the typical food processing conditions, e.g., thermal processing in high temperatures, and can thus be found not only in fresh but also in processed foods (Raters and Matissek, 2008). There are five main groups of mycotoxins that occur in food: aflatoxins, fumonisins, ochratoxin, deoxynivalenol/nivalenol, and zearalenone (Tola and Kebede, 2016). Aflatoxins are ranked as the most toxic and deadly naturally occurring substances. Amongst them aflatoxin B1 (AFB₁) has been ranked as the most carcinogenic and toxic substance produced by fungi and categorized as carcinogenic to humans according to the International Agency for Research on Cancer (IARC) (Rushing and Selim, 2019). Fumonisin, and especially their main representative fumonisin B1 (FB₁) are not as toxic as aflatoxins; nonetheless they have been classified as Class 2B carcinogens (possibly carcinogenic to humans) by the IARC (Reddy et al., 2010). Due to the severe effects on human health (carcinogenicity, hepatotoxicity, impairment of immune system, nephrotoxicity, teratogenicity, neurotoxicity and reproductive toxicity) associated with the consumption of food contaminated with mycotoxins, even in very low concentrations, there is a pressing need for sensitive and reliable methods for their detection. Moreover, food products prone to mycotoxins contamination should be checked to guarantee that food samples are in accordance with Commission Regulation (EC) No 1881/2006 of 19 December 2006, which sets, amongst other, maximum levels for mycotoxins in foodstuffs. This has motivated the development of several methods for the detection and/or quantification of mycotoxins, ranging from chromatographic to immunochemical ones (Turner et al., 2015; Chauhan et al., 2016; Anfossi et al., 2016; Rahman et al., 2019) which, however, are time and labor consuming and appropriate mainly for laboratory use. To satisfy the need for rapid PoN determinations without compromising the analytical performance, several optical (Mahmoudpour et al., 2019) and electrochemical sensing configurations (Goud et al., 2018) have been exploited using as recognition elements mainly antibodies but also synthetic receptors such as aptamers, molecularly imprinted molecules, etc. (Chauhan et al., 2016). Depending on the detection principle, most sensors offer simplicity, ease-to-use, short analysis time and portability; however, rarely all these features are combined with multi-analyte potential. The immunosensor developed based on MARS transducer for the simultaneous determination of AB₁ and FB₁ is based on a competitive immunoassay format. Therefore, the two mycotoxin-protein conjugates were immobilized onto the SiO₂ areas of different thickness and interrogated by a single reflection probe as mixtures of calibrators or samples with the two analyte specific antibodies are run over the transducer. The immunosensor developed combines the short analysis time, portability, and multi-analyte potential with the sensitivity required for detection of the two targeted mycotoxins in cereal samples.

2. Materials and methods

2.1. Materials and instruments

Mouse monoclonal antibodies against AFB₁ and FB₁, the AFB₁ conjugate with bovine serum albumin (AFB₁-BSA), and the FB₁ conjugate with ovalbumin (FB₁-OVA) were purchased from Aokin AG (Berlin, Germany). Aflatoxin B₁, Fumonisin B₁, (3-aminopropyl)triethoxysilane (APTES) and highly pure methanol, ethanol and acetonitrile (CHROMASOLV® for HPLC, $\geq 99.9\%$) were obtained from Sigma-Aldrich (St. Louis, MO). Bovine serum albumin (BSA) was purchased from Acros Organics (Geel, Belgium). Goat anti-mouse IgG (affinity purified) was from Merck Millipore (Darmstadt, Germany). The water used throughout the study was distilled.

The MARS measurement set-up shares several components with the standard WLRS set-up and consists of a) the optical module for the

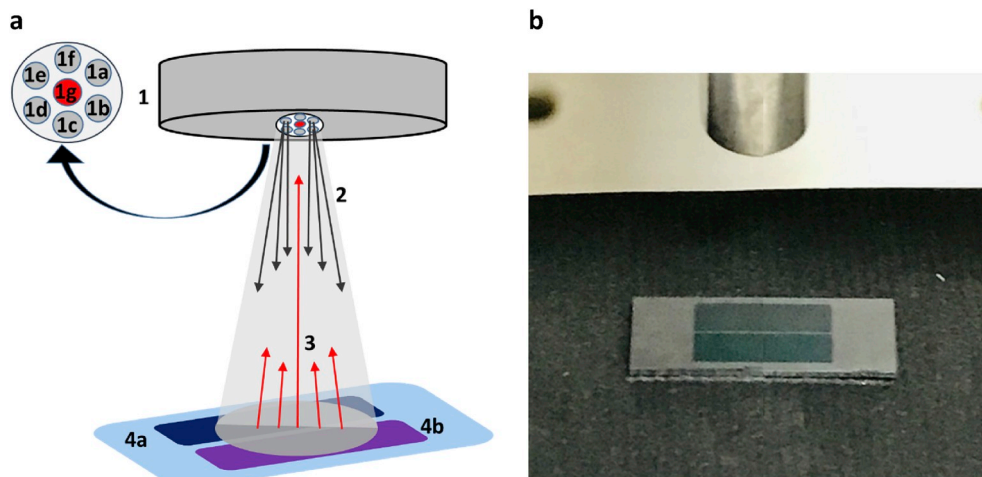


Fig. 1. (a) Schematic of MARS set-up for reflectance spectrum acquisition from chips with two SiO₂ areas of different thickness. Shown are: 1 the reflection probe with 1a-1f corresponding to fibers for incident light delivery to the chip surface and 1g to fiber for reflected light collection; 2 the incident light beam; 3 the reflected light; and 4a and 4b, the two sensing areas of SiO₂. (b) Image of the MARS chip with the two sensing areas under the reflection probe.

illumination of the biochip and the recording of the specular reflectance spectrum, b) the docking station for the placement of the biochip and c) the external fluidic circuit for the supply of the sample to be analyzed and the reagents required. In summary, the optical module of the MARS set-up consists of three elements: a visible-near infrared light halogen tungsten light source that guarantee long-term stable operation (ThetaMetrisis SA), a miniaturized USB controlled spectrometer (Ocean Optics Inc.) operating in the visible range, and a proprietary designed reflection probe (ThetaMetrisis SA) (see Fig. 1 and 2). The MARS biochip is the Si chip with the SiO₂ areas of different thicknesses (see Fig. 1b) covered by a custom designed microfluidic cell (Jobst Technologies GmbH, Freiburg, Germany) providing the fluidic connections to the solutions and the micropump. For the implementation of the assay and the facile monitoring of the biomolecular interactions, the biochip is inserted in an opaque docking station that provides for automatic alignment of the bioreactive zone to the reflection probe and at the same time allows for operation under ambient light conditions which is important for use of the device at the Point-of-Need. The reflected spectrum is recorded continuously (integration time 60 ms; averaging 15 times; 1 spectrum per second) from the spectrometer and processed by a dedicated application developed by ThetaMetrisis SA for the simultaneous monitoring of the bioreactions taking place on the two sensing areas of the MARS biochip. In particular, the software transforms in real-time the spectrum shifts to “effective biomolecular layer thickness” changes.

2.2. Preparation of calibrators and samples

Stock solutions of AFB₁ and FB₁ with concentration of 1 mg/mL were prepared in an 80:20 methanol/water mixture. These solutions were stored in aliquots at -20° C. Calibrators were prepared in a 80:20 (v/v) mixture of acetonitrile/water and kept aliquoted at 4 °C for up to 2 months. Grain samples (maize, wheat) were finely ground using a commercial grinder (Waring; Stamford, CT) and mixed for homogenization. Two grams of grounded sample were extracted with 10 mL of 80:20 (v/v) acetonitrile/water mixture under continuous shaking in an orbital shaker for 60 min. The extracts were then centrifuged at 5000 rpm for 5 min and the supernatant was collected. For the recovery experiments, 200 µL of solution with known concentration of the two mycotoxins was mixed with 2 gr of grounded sample and left to dry for 1 h at room temperature prior to extraction. Calibrators and sample extracts were diluted 20 times with assay buffer prior to analysis.

2.3. Biochip preparation and assay performance

Chips were cleaned/hydrophilized by immersion in a 1:1 H₂SO₄/H₂O₂ (30% v/v) mixture for 30 min. After thorough washing with distilled water, the chips were dried with N₂ and immersed for 20 min in a 2% (v/v) APTES solution. Chips were then washed with distilled water and thermally cured at 120 °C for 20 min. The SiO₂ areas of different thickness of the chips were spotted with mycotoxins-protein conjugates (100 µg/ml in 0.05 M carbonate buffer, pH 9.2) using the BioOdyssey Calligrapher Mini Arrayer (Bio-Rad Laboratories, Inc.). Coverage of the desired chip areas was achieved by deposition of multiple overlapping spots (each one of ~400 µm in diameter). During spotting the humidity was set at 75% and the temperature at 15 °C to avoid drying of the deposited solution, whereas after spotting the chips were incubated overnight at RT and 75% humidity. The chips were rinsed with washing buffer (10 mM Tris-HCl, pH 8.25, 0.9% NaCl), blocked with immersion for 1 h in 1% (w/v) BSA solution in 0.1 M NaHCO₃, pH 8.5, rinsed with washing buffer and distilled water, and dried with N₂. The functionalized chips (referred hereinafter as biochips) were used either immediately or kept at 4 °C in a desiccator until use. Prior to assay, each biochip was assembled with the fluidic module, placed on the docking station and equilibrated with assay buffer (50 mM Tris-HCl, pH 7.8, 9 g/L NaCl, 5 g/L BSA, 0.5 g/L NaN₃). Then, 1:1 vol mixtures of the calibrators or the samples with the antibodies (1.5 µg/mL of anti-AFB₁ mAb and 0.5 µg/mL of anti-FB₁ Mab in assay buffer) were run over the chip for 7 min at a flow rate of 30 µL/min. After that, a 10 µg/ml solution of goat-anti-mouse IgG in assay buffer was flowed for 5 min at the same flow rate. The biochip was then regenerated by passing 100 mM HCl solution for 3 min and equilibrated with assay buffer. For the preparation of the calibration curves, the “effective biomolecular layer thickness” values obtained for the different calibrators (S_x) were expressed as percent ratios of the thickness corresponding to zero calibrator (S₀) and plotted versus each mycotoxin concentration in the calibrators in linear/log scale.

3. Results and discussion

3.1. MARS principle of operation

In standard WRLS methodology the transducer is a Si die with 1.0 µm thick uniform thermally grown SiO₂ layer. The reflectance spectrum as recorded by a spectrometer in the visible range is illustrated in Fig. 2a where the interference extrema (maxima and minima) are clearly

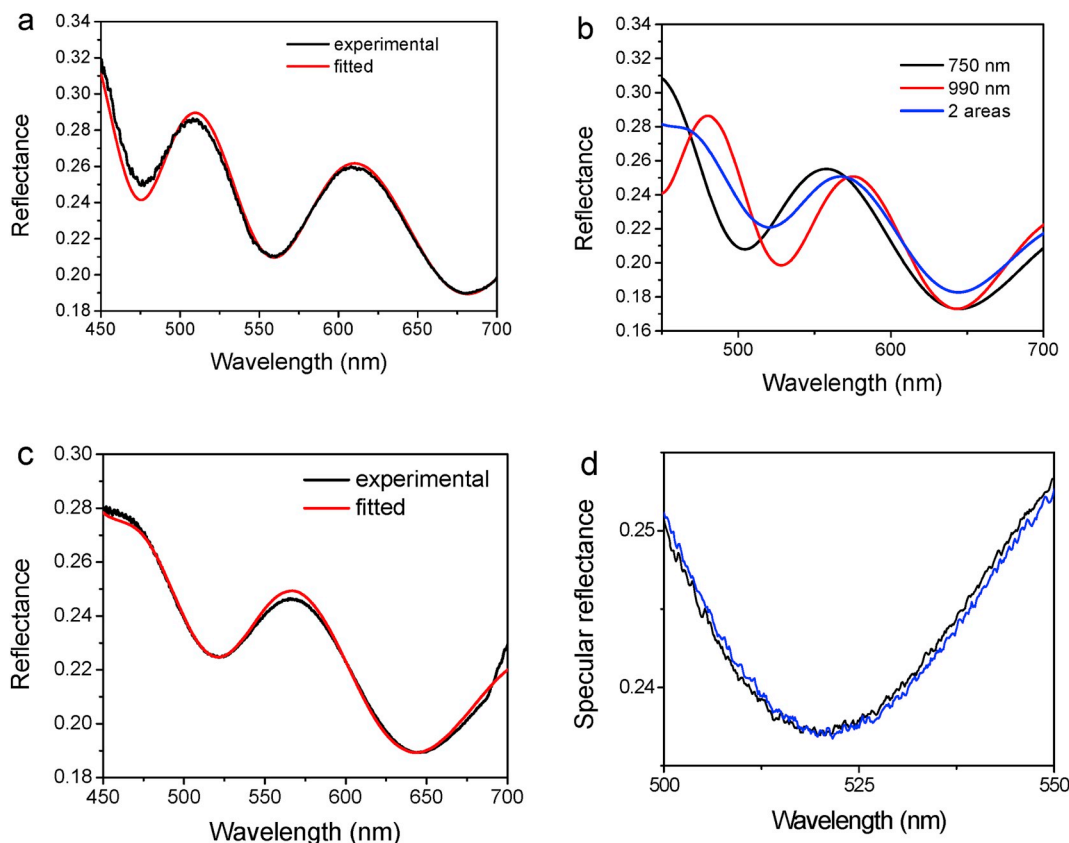


Fig. 2. (a) Reflectance and fitted spectrum from a WLRs chip with a 1- μm thick SiO_2 layer. (b) Theoretical reflectance spectra from a MARS chip with 2 areas of SiO_2 with thickness of 750 and 990 nm. (c) Reflectance and fitted spectrum for MARS chips with 2 areas of SiO_2 with thickness of 750 and 990 nm. (d) Experimental reflectance spectrum in the 500–550 nm spectral region prior (black line) and after a bioreaction (blue line) performed in a MARS chip with 2 areas of SiO_2 with thickness of 750 and 990 nm. All experimental spectra have been obtained with the fluidic on top of the chip filled with assay buffer. (For interpretation of the references to colour in this figure legend, the reader is referred to the Web version of this article.)

shown. In MARS methodology there are two sensing areas on the same Si chip and each sensing area has a different SiO_2 thickness. If those two areas are individually probed the extrema are different in number and are located at different wavelengths, as it is illustrated in Fig. 2b for areas with SiO_2 thickness of 750 (black line) and 990 nm (red line). When these two sensing areas are close to each other, then by appropriately designed reflection probe is possible to acquire the reflectance from both areas. Such a theoretical reflectance spectrum is also illustrated in Fig. 2b (blue line). Then by executing fitting with the sum of the two interference equations it is possible to measure the thickness of each SiO_2 area, without the need of equal contribution from both sensing areas in the total reflectance signal. In MARS methodology by applying the Levenberg-Marquart algorithm it is possible to measure in real-time the effective biomolecular adlayer thicknesses of both sensing areas. In Fig. 2c, the experimental reflectance spectrum from a MARS chip in buffer solution is illustrated along with the fitted one, while in Fig. 2d, the reflectance spectrum of the same chip prior to and after the growth of a biomolecular layer resulting from the same bioreaction is shown. As shown, the growth of this biomolecular layer causes a red spectral shift which the developed software transforms to effective biomolecular adlayer thickness.

3.2. Selection of silicon dioxide thicknesses combination

The fabrication of the MARS chip was performed by repetitive optical lithography, etching and thermal oxidation steps in order to create closely spaced areas of SiO_2 with different thicknesses on top of the Si wafer. Following this process, chips with two SiO_2 areas with nominal thickness of 550/770, 990/1170, 750/990 and 1190/1420 nm, have

been fabricated. The repeatability of the fabrication procedure was tested through determination of the SiO_2 thickness at each area using the WLRs set-up. In total, 12 chips from two batches have been tested and the mean values of thicknesses \pm SD determined were: 527 ± 2 nm (0.5%), 774 ± 2 nm (0.3%); 996 ± 3 nm (0.3%), 1175 ± 2 nm (0.1%); 711 ± 2 nm (0.3%), 984 ± 5 nm (0.5%); and 1198 ± 5 nm (0.5%), 1389 ± 2 nm (0.2%). Although the determined thickness values deviate slightly from the nominal ones, the thickness repeatability from chip to chip and batch to batch was very high with coefficients of variation $\leq 0.5\%$ for all SiO_2 thicknesses.

Once the repeatability with respect to SiO_2 layer thickness of the two sensing areas per chip was determined, the effect of the SiO_2 thickness on the response obtained during the immunoassay was studied. Therefore, chips with all the combinations of 2 SiO_2 areas with nominal thickness of 550/770, 990/1170, 750/990 and 1190/1420 nm, have been tested after biofunctionalization of both areas with the same mycotoxin-protein conjugate. The responses obtained from each one of the SiO_2 areas for the zero calibrator of the FB_1 assay are provided in Fig. S1. As shown, the responses obtained from the areas with SiO_2 thickness equal to or higher than 750 nm were identical with mean value \pm SD of 0.94 ± 0.02 (%CV = 2.06). Based on these results, the combination 750–990 was selected in order to reduce as possible the time and cost for the chips fabrication, since the creation of thicker SiO_2 layer requires longer thermal oxidation steps.

3.3. Development of single-analyte immunosensor

Prior to development of dual-analyte assay, the assays for AFB_1 and FB_1 have been separately optimized in the WLRs platform. Aiming to a

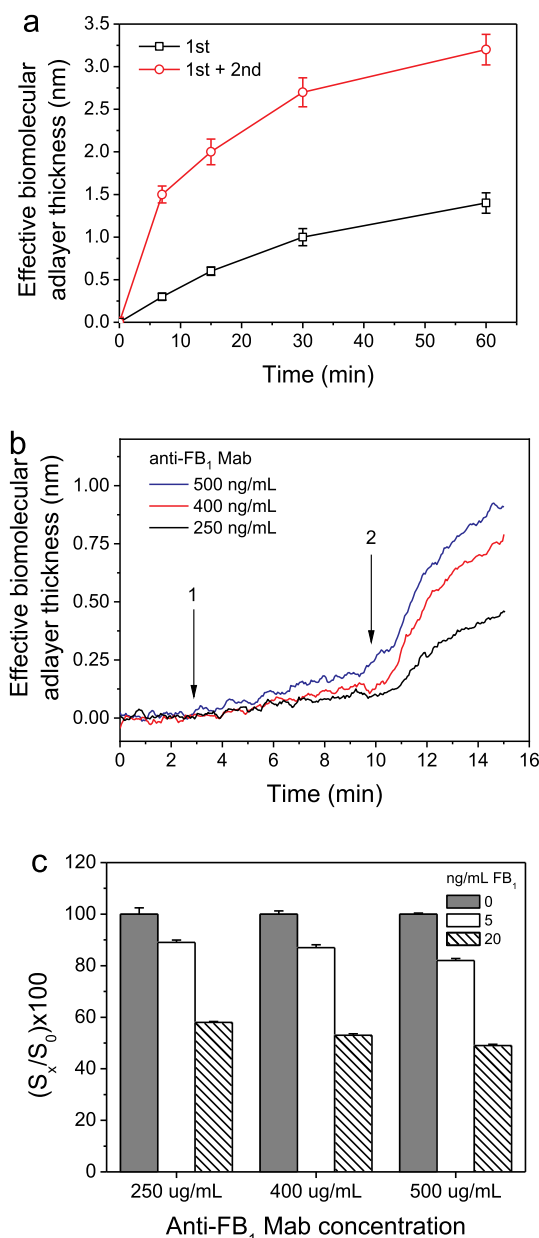


Fig. 3. (a) Evolution with time of signal for AFB₁ zero calibrator obtained only from the 1st immunoreaction step (black line) or from the 1st immunoreaction followed with a 5-min reaction with the secondary antibody (red line). (b) Real-time responses obtained for the FB₁ zero calibrator using 250 (black line), 400 (red line), and 500 ng/mL (blue line) anti-FB₁ Mab. The first arrow indicates the introduction of zero calibrator/anti-FB₁ Mab mixture and the second of secondary antibody solution. (c) Percent signal with respect to zero calibrator (gray bars) obtained for calibrators containing 5 (white bars) or 20 ng/mL FB₁ (striped bars). Each point is the mean value of three measurements \pm SD. (For interpretation of the references to colour in this figure legend, the reader is referred to the Web version of this article.)

device for PoN application, the assay duration should be as short as possible, therefore the first parameter studied was the duration of the two immunoreaction steps, namely the reaction of the mycotoxin-specific Mabs with the immobilized onto the chip mycotoxin-protein conjugate (1st immunoreaction) and the reaction of the secondary antibody with the immunosorbed Mabs (2nd immunoreaction). As shown in Fig. 3a for the AFB₁ assay, the signal obtained for the zero calibrator from the 1st immunoreaction step (black line) reaches values equal to or higher than 1 nm after at least 30 min of reaction. On the

other hand, the introduction of a 5-min reaction with the secondary antibody resulted in zero calibrator signal value of approx. 1.4 nm for 7-min duration of the 1st immunoreaction step. It should be noted that the signal obtained for a 5-min reaction with the secondary antibody corresponded to more than 50% of the maximum plateau signal value, which was achieved after 60-min reaction with the secondary antibody (see Fig. S2a of Supplementary material). Similar results were obtained for the FB₁ assay, for which a zero calibrator signal of approx. 1 nm was obtained for 1st and 2nd immunoassay step duration of 7 and 5 min, respectively (Figs. S2b and S2c, Supplementary material).

The concentration of mycotoxin-protein conjugate used for chip coating and the concentration of antibody were optimized with respect to zero calibrator signal and the assay sensitivity as it was defined by the percent signal drop achieved for calibrators containing fixed amount of the two mycotoxins with respect to zero calibrator. As shown in Fig. 3b & 3c, regarding the FB₁ assay, for a fixed conjugate concentration used for coating, increase of anti-FB₁ antibody concentration resulted in increase of the analytical signal without affecting the assay sensitivity. Similar results are provided for AFB₁ in Fig. S3 of Supplementary material. The combinations of conjugate/Mab finally selected were 100 μ g/mL/0.5 μ g/mL for FB₁ and 100 μ g/mL/1.5 μ g/mL for AFB₁.

3.4. Development and evaluation of dual-analyte immunosensor

Once the single analyte immunoassay conditions were established, the dual-analyte was developed using chips with 2-areas of SiO₂ each one modified with the protein-conjugate of AFB₁ or FB₁. For the assay, mixtures of calibrators containing both mycotoxins and the respective specific antibodies were run over the chips followed by reaction with secondary antibody, as is depicted in Fig. 4a. A typical response obtained upon running the zero calibrator/Mabs mixture over the dual-analyte chip is provided in Fig. 4b. The lack of cross-reactivity of each antibody towards the other analyte was demonstrated by running separately, over a chip on which each of the SiO₂ areas was functionalized with a different mycotoxin-protein conjugate, solutions of each specific antibody. As shown in Fig. 4c–d, no measurable response was obtained from the area coated with one analyte conjugate when the Mab for the other analyte was run over the chip. The lack of cross-reactivity was also confirmed by the fact that the calibration curves obtained with the dual-analyte sensor were identical to those obtained from single-analyte sensors for the determination of AFB₁ (Fig. 5a) and FB₁ (Fig. 5b), respectively. In addition, in order to demonstrate the lack of non-specific binding, mixtures of the mycotoxins Mabs were run over a chip with two sensing areas of SiO₂ non-coated with the mycotoxin conjugates but blocked with BSA. As shown in Fig. S4 of Supplementary material, there was not any measurable response from both areas, indicating the lack of non-specific binding.

From the calibration curves presented in Fig. 5a and b, the assays limit of detection (LOD) was determined as the concentration corresponding to signal equal to mean value of 10 replicate measurements of zero calibrator -3 SD and it was found to be 0.05 ng/mL for AFB₁ and 1.0 ng/mL for FB₁. Similarly, the quantification limits were determined as the concentration corresponding to mean value -10 SD of 10 replicate measurements of zero calibrator and were 0.15 and 3.3 ng/mL for AFB₁ and FB₁, respectively, whereas the linear response ranges extended up to 5.0 and 50 ng/mL, respectively. These quantification limits correspond to 5.0 and 100 ppb in grounded maize/wheat when a 10-times dilution of extracts is adopted. Taking into account that according to EU legislation, the maximum levels (MLs) in μ g/kg or ppb for AFB₁ for maize destined for human consumption are 5.0 ppb, while for FB₁ in unprocessed maize and maize based cereals and snacks are 800 and 4000 ppb, respectively, the proposed sensor is suitable for the determination of the two mycotoxins in whole grain samples as well as in processed cereal products.

The sensor was also evaluated for the determination of the two mycotoxins in whole grain samples (wheat and maize). The extraction

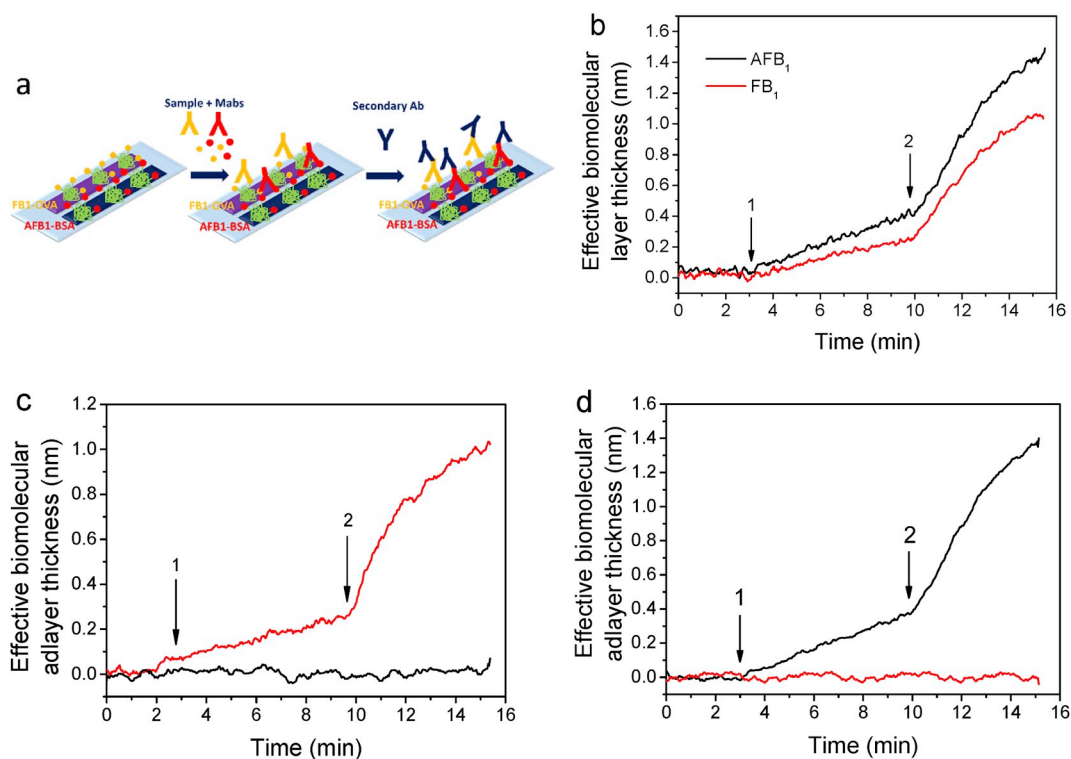


Fig. 4. (a) Schematic of the dual-analyte immunoassay steps. (b) Real-time response corresponding to zero calibrator of AFB₁ (black line) and FB₁ (red line) obtained from a dual-analyte chip. (c, d) Real-time responses obtained from a dual-analyte chip when running over (c) a mixture of zero calibrator with anti-FB₁ Mab or (d) a mixture of zero calibrator with anti-AFB₁ Mab. Black lines correspond to response from the area functionalized with the AFB₁-BSA conjugate and red lines from the area functionalized with the FB₁-OVA conjugate. Arrow 1 indicates the introduction of calibrator/specific Mabs mixture and arrow 2 the introduction of secondary antibody. (For interpretation of the references to colour in this figure legend, the reader is referred to the Web version of this article.)

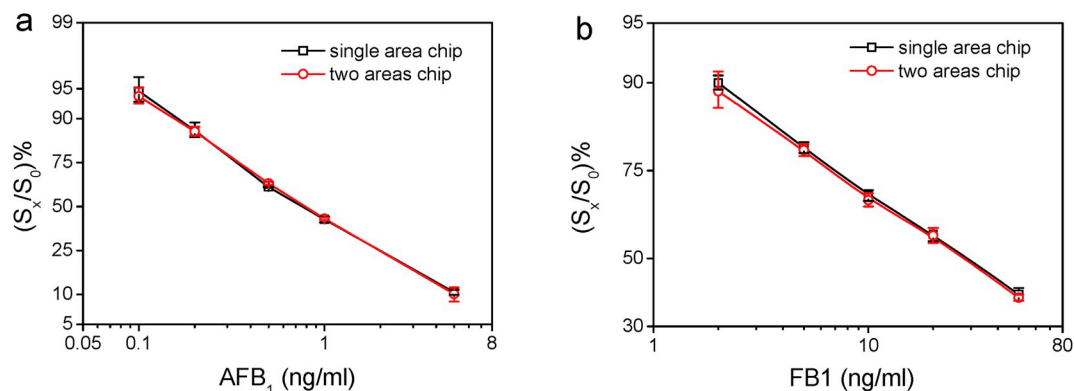


Fig. 5. AFB₁ (a) and FB₁ (b) calibration curves obtained from a single area chip with SiO₂ thickness of 1 μ m (black squares) or from a two-area chip where the one area was functionalized with AFB₁-BSA conjugate and the other with FB₁-OVA conjugate (red circles). (For interpretation of the references to colour in this figure legend, the reader is referred to the Web version of this article.)

protocol was optimized through ELISA experiments and recoveries ranging from 88 to 109% have been determined in spiked samples when an 80:20 acetonitrile/water mixture was employed. Thus, prior to application in cereal samples analysis, the effect of acetonitrile to the assay performance was determined. As shown in Fig. S5, both assays could tolerate up to 10% (v/v) acetonitrile in the assay buffer used for the preparation of calibration. Moreover, the calibration curves obtained for up to 10% (v/v) acetonitrile were identical to those obtained for both analytes without acetonitrile in the calibrators' buffer (data not shown). The extraction procedure was applied to wheat and maize samples containing non-detectable quantities of the two mycotoxins prior to and after the addition of known amounts of the two mycotoxins. In all cases, a 20-time dilution of the extracted samples was applied. The

results presented in Table S1 show that the recovery values ranged from 85 to 115%, verifying the accuracy of the determinations.

3.5. Comparison with other optical label-free immunosensors

The performance of our immunosensor regarding the simultaneous determination of AFB₁ and FB₁ was compared in terms of detection sensitivity, dynamic range and analysis time to that of other label-free optical immunosensors reported the last few years (2016–2019) for the detection of the two targeted mycotoxins. The comparison data are provided in Table 1. As shown most reports refer to single analyte determinations mainly of AFB₁, while there are only four reports concerning the simultaneous determination of AFB₁ and FB₁, combined

Table 1Comparison of the dual-analyte sensor developed with literature optical sensors for the determination of AFB₁/FB₁.

Sensing principle	Analytes determined	LOD (ng/mL or ng/gr)	Dynamic range (ng/mL)	Assay duration	Sample type	Ref #
Proposed	AFB ₁ /FB ₁	0.05/1.0	0.1–5.0/2.0–50	12 min	maize & wheat	
SRP (3-plex)	AB ₁ /FB ₁	0.6/2.0	3.0–260/10–1200	4 min	barley	Joshi et al. (2016)
iSPR (6-plex)	AFB ₁ /FB ₁	10/13	38–8000/48–3800	4 min	barley	Joshi et al. (2016)
SPR	AFB ₁	0.125	0.125–62.5	2 min	wine & beer	Sun et al. (2017)
SPR	AFB ₁	0.19	1.5–50	2 min	vinegar	Wu et al. (2018)
SPR	AFB ₁ (OTA/ZEN/DON)	0.59	0.99–21.92	15 min	maize & wheat	Wei et al. (2019)
SPR portable	AFB ₁	2.51	16–200	~5 min	rice, peanut, & almond	Moon et al. (2018)
LSPR	AFB ₁	0.0002	0.003–3.12	30 min	maize	Park et al. (2017)
TIRE/LSPR	AFB ₁	0.01	up to 10	10–15 min	buffer	Nabok et al. (2019)
OWLS	AFB ₁	–	0.1–100	5–7 min	paprika	Majer-Baranyi et al. (2016)
OWLS	AFB ₁	–	0.01–10	n.d.	paprika	Adányi et al., 2018
MZI	AFB ₁ /FB ₁ (DON)	0.1/0.7	0.2–5.0/1.4–25	12 min	beer	Pagkali et al. (2018)
SCI	AFB ₁	1.0	up to 12	30 min	white wine	Orlov et al. (2017)
PI-OPW	AFB ₁	0.0007	0.01–100	40 min	buffer	Al-Jawdah et al. (2019)

with the determination of other mycotoxins in some cases. The comparison with classical SPR (Joshi et al., 2016; Sun et al., 2017; Wu et al., 2018; Wei et al., 2019; Moon et al., 2018) reveals that the proposed immunosensor provided lower or similar limits of detection, while localized SPR (LSPR) results in much lower detection limits for assay times that are equal or higher than that of the proposed sensor (Park et al., 2017; Nabok et al., 2019). Nonetheless, both LSPR sensors are single-analyte devices relying on rather bulky optical set-ups. AFB₁ has also been determined using sensors based on optical waveguide light-mode spectroscopy (OWLS) (Majer-Baranyi et al., 2016; Adányi et al., 2018). The limits of quantification reported are greatly improved when the sensor surface was modified with gold nanoparticles (Adányi et al., 2018). Although OWLS is a sensing principle that has been commercialized, there are no instruments appropriate for on-site use. In addition, OWLS requires temperature control of the sensing element, while no temperature control is required for the proposed sensor. The proposed sensor exhibits comparable limits of detection/quantification with an immunosensor based on Mach-Zehnder interferometers (MZIs) integrated onto silicon chips (Pagkali et al., 2018). A sensor based on spectral-correlation interferometry (SCI) has been also evaluated with respect to AFB₁ determination (Orlov et al., 2017). The particular sensor demonstrates a twenty-time higher limit of detection as compared to the proposed sensor for an assay duration twice longer than that of the proposed one. Finally, comparison of the proposed sensor with a sensor built on a SiO₂-Si₃N₄-SiO₂ optical planar waveguide (OPW) operating as a polarization interferometer (PI) (Al-Jawdah et al., 2019), reveals a 10-time lower quantification limit with respect to the proposed sensor; achieved, nonetheless in 3-fold longer assay duration and demonstrated only for calibrators prepared in buffer. Overall, the proposed sensor offers the ability to detect simultaneously AFB₁ and FB₁ in cereals and cereal-derived products at concentrations in the range of the MLs set by EU. The assay duration is relatively short (12 min) and the necessary instrumentation can be miniaturized through inclusion of both optical and fluidic components to a compact device since neither temperature nor external light fluctuations affect the recorded signal.

4. Conclusions

The development of a dual-analyte immunosensor for the rapid and sensitive determination of two mycotoxins, AFB₁ and FB₁, in wheat and maize samples has been demonstrated. The sensor is based on transducers with 3-D structuring of a SiO₂ layer on a Si substrate that enables the monitoring of multiple bioreactions with a single reflection probe and without any moving parts through a novel sensing principle that of Multi Area Reflectance Spectroscopy (MARS). The advantage of MARS methodology relies on the fact that the transducers are fabricated with mainstream microelectronics technology (standard optical lithography, etching and thermal oxidation) allowing for the realization of chips with closely spaced sensing areas of different but well-defined thicknesses on

the Si wafer. In the current work, each one of the sensing areas was functionalized with a mycotoxin-protein conjugate aiming to simultaneous determination of AFB₁ and FB₁. It was found that the dual-analyte assays had identical analytical characteristics with the respective single-analyte ones. The detection limits achieved were 0.05 ng/mL for AFB₁ and 1.0 ng/mL for FB₁, with dynamic ranges extending up to 5.0 and 50 ng/mL, respectively. For the determination of the two mycotoxins in whole grain samples (wheat and maize) an optimized extraction protocol was applied and recoveries of exogenous added mycotoxins ranging from 85 to 115% were achieved. Taking into account the analytical performance of the immunosensor developed and the lack of moving parts that allows for multiplexed determinations without affecting the instrument size, the proposed sensing format is expected to considerably facilitate the built-up of portable devices for application at the point-of-need.

Author contribution

V. Anastasiadis: Investigation; Data curation.
 G. Koukouvinos: Formal analysis; Visualization.
 P.S. Petrou: Conceptualization; Supervision; Writing original draft, review & editing.
 A. Economou: Writing - review & editing;
 J. Dekker: Resources; Validation;
 M. Harjanne: Resources; Validation;
 P. Heimala: Funding acquisition; Writing - original draft.
 D. Goustouridis: Conceptualization; Software; Validation.
 I. Raptis: Conceptualization; Project administration, Resources; Funding acquisition Writing - original draft, review & editing.
 S.E. Kakabakos: Supervision; Funding acquisition; Writing - review & editing.

Declaration of competing interest

The authors declare that they have no known competing financial interests or personal relationships that could have appeared to influence the work reported in this paper.

Acknowledgement

We acknowledge support of this work by the project “NCSRDI-NRSTES research activities in the framework of the national RIS3” (MIS 5002559) which is implemented under the “Action for the Strategic Development on the Research and Technological Sector”, funded by the Operational Programme “Competitiveness, Entrepreneurship and Innovation” (NSRF 2014–2020) and co-financed by Greece and the European Union (European Regional Development Fund). This work was partially supported by EU project ACTPHAST (Grant Agreement No. 619205). We would like to thank ATPr&d S.r.l. (Via Ca’ Marzare, 3, 36043 Camisano

Vicentino, Italy) for providing cereal samples with no detectable levels of AFB₁ and FB₁ as determined by an external laboratory.

Appendix A. Supplementary data

Supplementary data to this article can be found online at <https://doi.org/10.1016/j.bios.2020.112035>.

References

- Adányi, N., Nagy, A.G., Takács, B., Szendrő, I., Szakacs, G., Szűcs, R., Tóth-Szeles, E., Lagzi, I., Weiser, D., Bóday, V., Sátorhelyi, P., Erdélyi, B., 2018. Sensitivity enhancement for mycotoxin determination by optical waveguide lightmode spectroscopy using gold nanoparticles of different size and origin. *Food Chem.* 267, 10–14.
- Al-Jawdah, A., Nabok, A., Abu-Ali, H., Catanante, G., Marty, J.-L., Szekecs, A., 2019. Highly sensitive label-free in vitro detection of aflatoxin B1 in an aptamer assay using optical planar waveguide operating as a polarization interferometer. *Anal. Bioanal. Chem.* <https://doi.org/10.1007/s00216-019-02033-4>.
- Anfossi, L., Giovannoli, C., Baggiani, C., 2016. Mycotoxin detection. *Curr. Opin. Biotechnol.* 37, 120–126.
- Arshavsky-Graham, S., Massad-Ivanir, N., Segal, E., Weiss, S., 2019. Porous silicon-based photonic biosensors: current status and emerging applications. *Anal. Chem.* 91, 441–467.
- Berthiller, F., Crews, C., Dall'Asta, C., De Saeger, S., Haesaert, G., Karlovsky, P., Oswald, I.P., Seefelder, W., Speijers, G., Stroka, J., 2013. Masked mycotoxins: a review. *Mol. Nutr. Food Res.* 57, 165–186.
- Bleher, O., Schindler, A., Yin, M.-X., Holmes, A.B., Luppá, P.B., Gauglitz, G., Proll, G., 2014. Development of a new parallelized, optical biosensor platform for label-free detection of autoimmunity-related antibodies. *Anal. Bioanal. Chem.* 406, 3305–3314.
- Chauhan, R., Singh, J., Sachdev, T., Basu, T., Malhotra, B.D., 2016. Recent advances in mycotoxins detection. *Biosens. Bioelectron.* 81, 532–545.
- Chen, Y., Liu, J., Yang, Z., Wilkinson, J.S., Zhou, X., 2019. Optical biosensors based on refractometric sensing schemes: a review. *Biosens. Bioelectron.* 144, 111693.
- Goud, K.Y., Kailasa, S.K., Kumar, V., Tsang, Y.F., Lee, S.E., Gobi, K.V., Kim, K.-H., 2018. Progress on nanostructured electrochemical sensors and their recognition elements for detection of mycotoxins: a review. *Biosens. Bioelectron.* 121, 205–222.
- Joshi, S., Segarra-Fas, A., Peters, J., Zuilhof, H., van Beek, T.A., Nielen, M.W.F., 2016. Multiplex surface plasmon resonance biosensing and its transferability towards imaging nanoplasmonics for detection of mycotoxins in barley. *Analyst* 141, 1307–1318.
- Kamat, V., Rafique, A., 2017. Designing binding kinetic assay on the bio-layer interferometry (BLI) biosensor to characterize antibody-antigen interactions. *Anal. Biochem.* 536, 16–31.
- Kozma, P., Kehl, F., Ehrentreich-Förster, E., Stamm, C., Bier, F.F., 2014. Integrated planar optical waveguide interferometer biosensors: a comparative review. *Biosens. Bioelectron.* 58, 287–307.
- Koukouvinos, G., Petrou, P.S., Misiakos, K., Drygiannakis, D., Raptis, I., Goustouridis, D., Kakabakos, S.E., 2015. A label-free flow-through immunosensor for determination of total- and free-PSA in human serum samples based on white-light reflectance spectroscopy. *Sens. Actuators B* 209, 1041–1048.
- Koukouvinos, G., Petrou, P., Misiakos, K., Drygiannakis, D., Raptis, I., Stefanitsis, G., Martini, S., Nikita, D., Goustouridis, D., Moser, I., Jobst, G., Kakabakos, S.E., 2016. Simultaneous determination of CRP and D-dimer in human blood plasma samples with white light reflectance spectroscopy. *Biosens. Bioelectron.* 84, 89–96.
- Koukouvinos, G., Petrou, P., Goustouridis, D., Misiakos, K., Kakabakos, S., Raptis, I., 2017a. Development and bioanalytical applications of a white light reflectance spectroscopy label-free sensing platform. *Biosensors* 7, 46.
- Koukouvinos, G., Tsiaila, Z., Petrou, P.S., Misiakos, K., Goustouridis, D., Ucles Moreno, A., Fernandez-Alba, A.R., Raptis, I., Kakabakos, S.E., 2017b. Fast simultaneous detection of three pesticides by a white light reflectance spectroscopy sensing platform. *Sens. Actuators B* 238, 1214–1223.
- Koukouvinos, G., Goustouridis, D., Misiakos, K., Kakabakos, S., Raptis, I., Petrou, P., 2018. Rapid C-reactive protein determination in whole blood with a white light reflectance spectroscopy label-free immunosensor for point-of-care applications. *Sens. Actuators B* 260, 282–288.
- Mahmoudpour, M., Dolatabadi, J.E.N., Torbati, M., Tazehkand, A.P., Homayouni-Rad, A., Miguel de la Guardia, M., 2019. Nanomaterials and new biorecognition molecules based surface plasmon resonance biosensors for mycotoxin detection. *Biosens. Bioelectron.* 143, 111603.
- Majer-Baranyi, K., Zalán, Z., Mörtl, M., Juracek, J., Szendrő, I., András Székács, A., Adányi, N., 2016. Optical waveguide lightmode spectroscopy technique-based immunosensor development for aflatoxin B1 determination in spice paprika samples. *Food Chem.* 211, 972–977.
- Makarona, E., Petrou, P., Kakabakos, S., Misiakos, K., Raptis, I., 2016. Point-of-Need bioanalytics based on planar optical interferometry. *Biotechnol. Adv.* 34, 209–233.
- Moon, J., Byun, J., Kim, H., Lim, E.-K., Jeong, J., Huang, J., Kang, T., 2018. On-site detection of aflatoxin B1 in grains by a palm-sized surface plasmon resonance sensor. *Sensors* 18, 598.
- Nabok, A., Al-Rubaye, A.G., Al-Jawdah, A.M., Tsgarodrska, A., Marty, J.-L., Catanante, G., Szekecs, A., Takacs, E., 2019. Novel optical biosensing technologies for detection of Mycotoxins. *Opt. Laser. Technol.* 109, 212–221.
- Orlov, A.V., Burenin, A.G., Massarskaya, N.G., Betin, A.V., Nikitin, M.P., Nikitin, P.I., 2017. Highly reproducible and sensitive detection of mycotoxins by label-free biosensors. *Sens. Actuators B* 246, 1080–1084.
- Pagkalis, V., Petrou, P.S., Makarona, E., Peters, J., Haasnoot, W., Jobst, G., Moser, I., Gajos, K., Budkowski, A., Anastasios Economou, A., Misiakos, K., Raptis, I., Kakabakos, S.E., 2018. Simultaneous determination of aflatoxin B1, fumonisin B1 and deoxynivalenol in beer samples with a label-free monolithically integrated optoelectronic biosensor. *J. Hazard Mater.* 359, 445–453.
- Park, J.-H.I., Byun, J.-Y., Jang, H., Hong, D., Kim, M.-G., 2017. A highly sensitive and widely adaptable plasmonic aptasensor using berberine for small-molecule detection. *Biosens. Bioelectron.* 97, 292–298.
- Rahman, H.U., Yue, X., Yu, Q., Xie, H., Zhang, W., Zhang, Q., Li, P., 2019. Specific antigen-based and emerging detection technologies of mycotoxins. *J. Sci. Food Agric.* 99, 4869–4877.
- Raters, M., Matissek, R., 2008. Thermal stability of aflatoxin B1 and ochratoxin A. *Mycotoxin Res.* 24, 130–134.
- Rau, S., Hilbig, U., Gauglitz, G., 2014. Label-free optical biosensor for detection and quantification of the non-steroidal anti-inflammatory drug diclofenac in milk without any sample pretreatment. *Anal. Bioanal. Chem.* 406, 3377–3386.
- Reddy, K.R.N., Salleh, B., Saad, B., Abbas, H.K., Abel, C.A., Shier, W.T., 2010. An overview of mycotoxin contamination in foods and its implications for human health. *Toxin Rev.* 29, 3–26.
- Rushing, B.R., Selim, M.I., 2019. Aflatoxin B1: a review on metabolism, toxicity, occurrence in food, occupational exposure, and detoxification methods. *Food Chem. Toxicol.* 124, 81–100.
- Stavra, E., Petrou, P.S., Koukouvinos, G., Kiritsis, C., Pirmettis, I., Papadopoulos, M., Goustouridis, D., Economou, A., Misiakos, K., Raptis, I., Kakabakos, S.E., 2018. Simultaneous determination of paraquat and atrazine in water samples with a white light reflectance spectroscopy biosensor. *J. Hazard Mater.* 359, 67–75.
- Sun, L., Wu, L., Zhao, Q., 2017. Aptamer based surface plasmon resonance sensor for aflatoxin B1. *Microchim. Acta* 184, 2605–2610.
- Tola, M., Kebede, B., 2016. Occurrence, importance and control of mycotoxins: a review. *Cogent Food Agriculture* 2, 1191103.
- Tsounidi, D., Koukouvinos, G., Petrou, P., Misiakos, K., Zisis, G., Goustouridis, D., Raptis, I., Kakabakos, S.E., 2019. Rapid and sensitive label-free determination of aflatoxin M1 levels in milk through a White Light Reflectance Spectroscopy immunosensor. *Sens. Actuators B* 282, 104–111.
- Turner, N.W., Bramhmbhatt, H., Szabo-Vezse, M., Poma, A., Coker, R., Piletsky, S.A., 2015. Analytical methods for determination of mycotoxins: an update (2009–2014). *Anal. Chim. Acta* 901, 12–33.
- Wei, T., Ren, P., Huang, L., Ouyang, Z., Wang, Z., Kong, X., Li, T., Yin, Y., Wu, Y., He, Q., 2019. Simultaneous detection of aflatoxin B1, ochratoxin A, zearalenone and deoxynivalenol in corn and wheat using surface plasmon resonance. *Food Chem.* 300, 125176.
- Wu, W., Zhu, Z., Li, B., Liu, Z., Jia, L., Zuo, L., Chen, L., Zhu, Z., Shan, G., Luo, S.-Z., 2018. A direct determination of AFBs in vinegar by aptamer-based surface plasmon resonance biosensor. *Toxicol.* 146, 24–30.
- Zhou, J., Qi, Q., Wang, C., Qian, Y., Liu, G., Wang, Y., Fu, L., 2019. Surface plasmon resonance (SPR) biosensors for food allergen detection in food matrices. *Biosens. Bioelectron.* 142, 111449.